Published in final edited form as:
Ultrasound Med Biol. 2007 November ; 33(11): 1805–1817.

Influence of the Cell Wall on Intracellular Delivery to Algal Cells by Electroporation and Sonication

Harold R. Azencott[1], **Gary F. Peter**[2,3], and **Mark R. Prausnitz**[1,*]

1 *School of Chemical & Biomolecular Engineering, Georgia Institute of Technology, Atlanta, GA30332*

2 *Institute for Paper Science and Technology, Atlanta, GA 30332*

3 *School of Forest Resources and Conservation, University of Florida, Gainesville, FL 32605*

Abstract

To assess the cell wall's role as a barrier to intracellular delivery, wild-type *Chlamydomonas reinhardtii* algal cells and mutant cells lacking a cell wall were exposed to electroporation or sonication. Flow cytometry determined intracellular uptake of calcein and bovine serum albumin (BSA) and loss of cell viability as functions of electroporation transmembrane potential and acoustic energy. Electroporation of wild-type cells increased calcein uptake with increasing transmembrane potential, but delivered much less BSA. Electroporation of wall-deficient cells had similar effects on calcein uptake, but increased BSA uptake as much as 7.5-fold relative to wild-type cells, which indicated that the cell wall was a significant barrier to BSA delivery during electroporation. Sonication of wild-type cells caused calcein and BSA uptake at similar levels. This suggests that the cell wall barrier to BSA delivery can be overcome by sonication. Increased electroporation transmembrane potential or acoustic energy also caused increased loss of cell viability, where wall-deficient cells were especially susceptible to lysis. Overall, we believe this is the first study to compare the effects of electroporation and sonication in a direct fashion in any cell type. Specifically, these findings suggest that electroporation primarily transports molecules across the plasma membrane, because its mechanism is specific to lipid bilayer disruption, whereas sonication transports molecules across both the plasma membrane and cell wall, because it non-specifically disrupts cell-surface barriers.

Keywords

cavitation; *Chlamydomonas reinhardtii*; electric field; electroporation; membrane disruption; ultrasound

INTRODUCTION

Since the advent of recombinant DNA technology in the 1970's, remarkable progress has been made in plant biotechnology (Birch 1997; Sharma et al. 2005). The greatest impact has been seen in the development of transgenic plants, as well as biopharmaceuticals and molecular pharming. Applications of plant biotechnology rely on methods to deliver genes and other macromolecules into cells. The dual barriers of the cell membrane and the cell wall found in

* Address editorial correspondence to Dr. Mark R. Prausnitz, School of Chemical & Biomolecular Engineering, Georgia Institute of Technology, 311 Ferst Drive, Atlanta, GA 30332-0100, Phone: (404) 894-5135, Fax: (404) 894-2291, Email: prausnitz@gatech.edu.

plant cells makes intracellular delivery difficult. This study sought to measure the relative importance of the cell wall as a rate-limiting barrier to intracellular delivery using algal cells at a model system.

Biological, chemical and physical methods have been developed to deliver macromolecules into plant cells. Delivery using agrobacterium as a biological vector has found success to deliver DNA into the nucleus of dicots (e.g., soybeans, tomatoes, squashes), but has difficulty delivering to monocots (e.g., rice, maize, wheat), does not deliver DNA to non-nuclear genomes, and does not deliver molecules other than DNA (Songstad et al. 1995). Chemical delivery agents, such as polyethylene glycol or liposomes (Gad et al. 1990), as well as the physical delivery method of electroporation (Nickoloff 1995), require the use of protoplasts, which are plant cells whose cell walls have been removed (Potrykus and Shillito 1986). The difficulty to regenerate mature plants from protoplasts has limited the utility of these methods. Finally, physical methods such as particle bombardment (gene gun) (Joersboe and Brunstedt 1990; Lui et al. 2006; Taylor and Fauquet 2002), as well as silicon carbide fibers (Kaeppler et al. 1990), microinjection (Neuhaus and Spangenberg 1990), and sonication (Trick and Finer 1997), have been successfully applied to intact plant cells, but often yield inefficient and variable gene expression. This previous work with sonication has emphasized the use of ultrasound to facilitate agrobacterium-mediated transformation, which contrasts with the direct and quantitative study of intracellular molecular uptake presented here.

To improve understanding of the barriers to intracellular delivery with the long-term goal of assisting applications in plant biotechnology, this study sought to more fully understand the role of the cell wall as a barrier to transport. We therefore exposed two algal cell strains – a wild-type strain, which has a cell wall, and a mutant strain, which lacks a cell wall – to two methods of intracellular delivery – electroporation, which is believed to act only on the cell membrane, and sonication, which is expected to act on both the cell membrane and cell wall – using two different molecules as uptake markers – calcein, which is a small molecule that should readily cross the cell wall, and bovine serum albumin (BSA), which is a macromolecule that should have difficulty crossing an intact cell wall. We were guided by the hypothesis that electroporation primarily transports molecules across cell membranes, because its mechanism is specific to lipid bilayer disruption, whereas sonication transports molecules across both cell membranes and cell walls, because it non-specifically disrupts cell-surface barriers.

As a secondary goal, we sought to assess the ability of sonication to deliver macromolecules into algal cells to motivate possible future studies to develop sonication as a biotechnology tool. We also sought to quantify the effects of sonication and electroporation on intracellular delivery and viability of algal cells, which has received only limited attention outside the context of gene transfection.

The model algal cells used in this study are two strains of *Chlamydomonas reinhardtii*, which is a widely studied unicellular green alga having a cell wall, a chloroplast, an “eye” that perceives light, and two anterior flagella (Harris 1989). We selected this species because its wild-type strain has a cell wall, but a mutant strain has been genetically altered to prevent synthesis of a cell wall (Hyams and Davies 1972). In this way, direct comparisons can be made between cells that differ essentially only by the presence or absence of a cell wall.

Although use of higher plant cells might be more directly relevant to biotechnology applications, we were unable to identify or develop unicellular higher plant cells that exist both with and without a cell wall. Protoplasts can be generated as wall-deficient, unicellular plant cells, but higher plant cells with intact cell walls exist primarily as multicellular colonies and cannot be easily separated into isolated cells (Knox 1992). Colonies are difficult to use because they are too big for analysis by flow cytometry and because their response to electroporation

and sonication is expected to differ from isolated cells (Canatella et al. 2004; Guzman et al. 2003).

Although algae have cell walls, they differ from higher plants. The walls of *C. reinhardtii* are made of glycoproteins containing an extensin-like protein rich in hydroxyproline and sugar residues including arabinose, galactose and mannose (Adair et al. 1987). Wall structure contains a central framework of polygonal plates bounded externally and internally by fibrous layers. In contrast, the walls of higher plants typically consist of a middle lamella, which is composed of pectic compounds and proteins and is shared by adjacent cells; a primary wall consisting of a rigid skeleton of cellulose microfibrils embedded in a gel-like matrix of pectic compounds, hemicellulose, and glycoproteins; and a secondary wall, which is extremely rigid and is made of cellulose, hemicellulose and lignin (Carpita and Gibeaut 1993).

Electroporation was selected as a delivery method because it is widely used and studied for delivery of DNA and other compounds to a broad variety of cell types, including plant cells (Nickoloff 1995) and specifically *C. reinhardtii* (Brown et al. 1991; Shimogawara et al. 1998), for which a quantitative mechanistic analysis has been published. Electroporation is believed to increase intracellular delivery by transiently disrupting cell membrane structure to form nanometer pores in the membrane that permit entry of macromolecules including DNA (Jaroszeski et al. 2000; Weaver and Chizmadzhev 1996). The mechanism is believed to be specific to lipid bilayers and has not been reported to transiently disrupt other biological barriers, such as cell walls. Unlike dielectric breakdown, which irreversibly disrupts membranes made of many materials, electroporation is a long-lived, but reversible, phenomenon that is believed to occur only in lipid bilayers due to the molecular rearrangements permitted by their fluid nature. For spherical cells of uniform size (such as *C. reinhardtii*), electroporation-mediated uptake is expected to be homogeneous across the cell population (Prausnitz et al. 1993). Applications of electroporation have primarily addressed biomedical problems, including extensive use for gene transfection in vitro and in vivo (Jaroszeski et al. 2000; Heller and Heller 2006), as well as enhanced chemotherapy of cancer in human patients (Mir et al. 2003).

Sonication was selected as the second delivery method for this study because it also has been shown to deliver macromolecules, including DNA, into cells, but is believed to act by a different mechanism (Miller et al. 1996). Although much less is known about sonication-mediated delivery, ultrasound is applied at conditions that cause cavitation, where the oscillation and collapse of cavitaiton bubbles is believed to mechanically break open cells in a manner that permits them to subsequently reseal (Schlicher et al. 2006). Mechanical effects of cavitation have been seen in many biological and non-biological structures, such as kidney stone destruction by lithotripsy and propeller pitting on submarines (Leighton 1994), suggesting that sonication's effects are probably not specific to cell membranes and might also disrupt cell walls. Intracellular delivery by sonication has been shown in mammalian cells to be heterogeneous, where levels of uptake vary widely within an exposed cell population (Guzman et al. 2001b). Applications of intracellular delivery using ultrasound have largely focused on biomedical needs, including drug and gene delivery studies in vitro and in vivo (Pitt et al. 2004; Bekeredjian et al. 2005; Paliwal and Mitragotri 2006).

MATERIALS AND METHODS

Cell Culture and Sample Preparation

Two strains of the green alga *C. reinhardtii* were obtained from the *Chlamydomonas* Genetic Center at Duke University (Durham, NC USA): the wild-type strain, CC-125, and a cell wall-deficient mutant strain, CC-3491 cw15 backcrossed 4X (CC-125 x CC-406). To prevent formation of multicellular colonies and thereby maintain a unicellular population, cell cycles

were synchronized by culturing under photosynthetic conditions with a cycle of 14 h of light followed by 10 h of darkness at 25 °C in 250 mL glass flasks containing acetate-free Sueoka's high-salt medium (Sigma Chemical, St. Louis, MO USA) (Sueoka 1960). Routine subculture was performed weekly by transferring 5 mL of the culture into 45 mL of fresh medium.

To prepare for exposure to electroporation or sonication, cell suspensions were removed from liquid culture 72 h after subculture and characterized in two ways. First, cell concentration was determined by Coulter counting (Coulter Multisizer II, Beckman Coulter, Fullerton, CA USA) and was typically in the range of 5×10^6 to 8×10^6 cells/mL. Second, the osmolarity of the growth medium was determined using a vapor-pressure osmometer (Model 5500; Wescor, Logan, UT USA) and was typically close to 80 mOsm.

Cells were then washed three times by centrifugation (950 *g*, 3000 rpm, 3 min, CS-15R centrifuge, Beckman Coulter) and resuspended at a final concentration of 10^6 cells/mL in phosphate-buffered saline (PBS, Mediatech, Herndon, VA USA) that had been previously diluted using deionized water from its stock osmolarity of 276 ± 10 mOsm to the osmolarity of the growth medium. Fluorescent tracer molecules, calcein or FITC-labeled BSA (Molecular Probes, Eugene, OR USA), were added from stock solutions to final concentrations, C_0, of 100 μM or 50 μM, respectively. Calcein is a negatively charged and biologically inert green-fluorescent molecule of molecular mass 623 Da and an estimated molecular radius of 0.6 nm (Edwards et al. 1995). FITC-labeled BSA is a negatively charged green-fluorescent molecule of molecular mass 66 kDa and an estimated molecular radius of 3.5 nm (Guzman et al. 2002).

Electroporation and Sonication

For electroporation experiments, 400 μL of the final cell suspension was pipetted into a 2-mm gap electroporation cuvette with embedded aluminum electrodes (BTX Model 620; Harvard Apparatus, Holliston, MA USA), which was placed in a high-voltage electric pulse generator (BTX Electro Cell Manipulator 600; Harvard Apparatus). The amplitude and duration of applied electric pulses were determined by monitoring pulser output on an oscilloscope (54603B; Hewlett-Packard, Colorado Springs, CO USA) using a 10:1 attenuating oscilloscope probe (HP 10071A; Hewlett-Packard).

Electroporation was achieved by applying two exponential-decay pulses with 1 ms time constants separated by a 30 s interpulse gap. Applied voltages were between 0 and 476 V. These correspond to nominal field strengths, E, between 0 and 2.38 kV/cm, which were calculated by dividing the applied voltage by the electrode spacing (2 mm). Maximum transmembrane potentials, U_{max}, were determined to be between 0 and 1.25 V using the relationship $U_{max} = 1.5\ r \cdot E$ (Foster and Schwann 1986), where average cell radii, r, of 3.5 μm and 4 μm for spherically shaped wild-type and wall-deficient cells, respectively, were determined by optical microscopy (IX70, Olympus, Melville, NY USA). It should be noted that U_{max} is the applied transmembrane potential, which adds to or subtracts from the cell's resting transmembrane potential. Because electroporation is known to be a strong function of transmembrane potential (Chang et al. 1992), this value is reported in this study, rather than the apparatus-dependent voltage or the cell size-dependent field strength. Negative control exposures (i.e., 0 V) were carried out in the same manner, except no electric pulse was applied to the sample.

For sonication experiments, the cell suspension was loaded into a 3-mL syringe with a 22-gauge needle (Becton Dickinson, Franklin Lakes, NJ USA) and injected into the sample chamber, which was made from a Sedi-Pet transfer pipette (Model 241, SAMCO, San Fernando, CA USA) whose stem had been cut to 2 cm in length. A meniscus was left at the top of the pipette stem and a 0.16-cm diameter stainless steel rod was inserted 2 mm into the

stem leaving a sample volume of approximately 1.4 mL. Overflow of solution was permitted to ensure that no visible air bubbles were trapped in the sample. The sample was then positioned at the axial and radial center of the ultrasound device transducer and exposed to the desired sonication conditions.

Sonication was carried out using an ultrasound device previously described and characterized (Liu et al. 1998; Cochran and Prausnitz 2001). Briefly, it was composed of a function generator, ultrasonic amplifier, matching transformer, and 4.5-cm inner-diameter, zirconate-titanate transducer resonant at 24 kHz. The cylindrical transducer formed part of the wall of a cylindrical chamber filled with deionized and partially degassed water to provide a coupling medium between the transducer and the sample. The water was degassed for 2 h using a bell jar (Nalgene, Rochester, NY USA) and vacuum pump (KNF Neuberger, Trenton, NJ USA) to remove bubble nucleation sites and thereby reduce cavitation in the water bath that could alter the pressure field in the sample chamber. The cell suspension was not degassed and therefore contained gas that could lead to cavitation. Indeed, previous characterization of this apparatus by acoustic spectrum and sonoluminescence analysis showed that extensive cavitation is induced during sonication at the conditions used in this study (Liu et al. 1998; Cochran and Prausnitz 2001).

Sonication exposures applied 24-kHz ultrasound at 304-kPa peak-to-peak pressure amplitude using 100-ms pulses at a 10% duty cycle. Pressure amplitudes were mapped as a function of position in the water bath using a calibrated hydrophone (Model 8103, Bruel and Kjaer, Norcross, GA USA). As described previously (Cochran and Prausnitz 2001), pressure amplitude varied by less than 20% within the volume of the sample chamber. Sonication time was varied from 80 to 1,300 pulses to achieve acoustic energy exposures between 25 and 400 J/cm^2. Energy exposure, E, was calculated using the formula

$$E = \frac{\left(\frac{P}{\sqrt{2}}\right)^2}{\rho c} t \quad (1)$$

where P is pressure (304 kPa), ρ is the density of water (1.0 kg/m^3), c is the speed of sound in water (1500 m/s), and t is exposure time (8 – 130 s). Energy exposures are reported in this study, because previous studies with other cell types found a broad correlation between cellular bioeffects and ultrasound energy exposure (Guzman et al. 2001a; Keyhani et al. 2001). Negative-control exposures (i.e., 0 J/cm^2) were carried out in the same manner, except no ultrasound was applied to the sample.

Analysis of Samples

After exposure to electroporation or sonication, cells were allowed to recover for 15 min at room temperature (22 °C) and then incubated on ice for an additional 20 – 90 min. Then, samples were washed three times by centrifugation (950 × g, 3 min, CS-15R centrifuge, Beckman Coulter) and resuspended in a final volume of 0.5 mL of fresh growth medium. Just before flow cytometry analysis, propidium iodide (Molecular Probes) was added to each sample at a final conentration of 0.1 mg/mL to label non-viable cells. Fluorescent beads (Polysciences, Warrington, PA USA) were also added at a concentration of 2.4 × 10^4 beads/mL to serve as a volumetric standard.

Following established methods (Canatella et al. 2001), flow cytometry (BD LSR, Becton Dickinson Biosciences, Franklin Lakes, NJ USA) was used to analyze approximately 20,000 cells from each sample, where cells were distinguished from debris on the basis of forward and side scatter. Non-fluorescent cells were interpreted as viable cells without uptake; green fluorescent cells were interpreted as viable cells with uptake of green-fluorescent calcein or

BSA; and red fluorescent cells were interpreted as non-viable cells labeled with propidium iodide. Cells were identified as 'fluorescent' if their fluorescence was greater than the background signal from 95% of untreated, control cells. Non-viable cells labeled with propidium iodide typically also had green fluorescence from calcein or BSA. We did not report this fluorescence, because intracellular uptake into non-viable cells is not relevant to this study. Finally, lysed cells were identified by subtracting the total (i.e., viable and non-viable) cell concentration in each sample from the total cell concentration in control samples. Computer analysis was performed using Windows Multiple Document Interface (WinMDI v. 2.8; TSRI Flow Cytometry, San Diego, CA USA).

Among viable cells with uptake, the number of molecules inside each cell was determined by calibrating the intensity of green fluorescence using fluorescein-based quantitative calibration beads (MESF, Flow Cytometry Standards Corporation, Fishers, IN USA). This calculation was facilitated by using a spectrofluorimeter (QuantaMaster, Photon Technology International, Brunswick, NJ USA) to determine the ratio of calcein and BSA fluorescence to fluorescein fluorescence, which was 0.67 ± 0.03 and 0.85 ± 0.02, respectively. Intracellular localization of fluorescence, rather than on the cell surface, was validated using confocal microscopy (LSM510, Carl Zeiss, Thorwood, NY USA). Intracellular concentrations, C, were calculated by dividing the average number of molecules per cell by the average cell volume of 180 or 268 μm^3 for wild-type or wall-deficient cells, respectively, as determined by optical microscopy (IX70, Olympus). In the figures, intracellular concentrations were nondimensionalized relative to the extracellular bath concentration, C_0.

Statistical Analysis

For all graphs presented in this study, each data point represents the mean of at least five replicates. Error bars are the standard errors of the means. When a comparison between two or more means was required, a Student's t-test or a one-way analysis of variance (ANOVA) with a 95% level of confidence was used where appropriate. When two factors were compared, a two-way ANOVA was used. A value of $p < 0.05$ was considered statistically significant. All statistical analyses were performed with StatView (v. 5.0.1, SAS Institute, Cary, NC USA).

RESULTS

Electroporation

This study sought to test the hypothesis that electroporation primarily transports molecules across cell membranes, because its mechanism is specific to lipid bilayer disruption, whereas sonication transports molecules across both cell membranes and cell walls, because it non-specifically disrupts cell-surface barriers. To test the first part of this hypothesis, we applied electric pulses to cause electroporation of two strains of the green alga, *Chlamydomonas reinhardtii*; the wild-type, which has an intact cell wall, and a mutant strain, which lacks a cell wall. We measured cell viability, as well as intracellular uptake of a small molecule (calcein, 623 Da) and a macromolecule (bovine serum albumin, 66 kDa). If our hypothesis is correct, calcein should be delivered into both cell strains to similar extents, because the small size of calcein permits its transport across an intact cell wall (Davis 1995), so that the cell membrane is the rate-limiting barrier. In contrast, BSA should be delivered into the wall-deficient mutant strain to a greater extent, because the large size of BSA prevents its transport across an intact cell wall, so that both the cell membrane and cell wall are rate-limiting barriers.

Considering calcein first, Figure 1A shows that calcein uptake increased with transmembrane potential for both cell strains (1-way ANOVA, $p<0.0001$), which is consistent with previously observed behavior in other cell types (Canatella et al. 2001; Gift and Weaver 1995). Of particular interest to this study, levels of calcein uptake were statistically the same in both cell

strains (2-way ANOVA, $p>0.05$), which is consistent with the expectation that the cell wall does not significantly impede transport of calcein. Figure 1A also shows that cell viability decreased with increasing transmembrane potential for both cell strains (1-way ANOVA, $p<0.0001$) and that the wall-deficient cells were generally more easily killed than the wild type (2-way ANOVA, $p<0.05$).

Considering BSA, Figure 1B shows that BSA uptake increased with transmembrane potential for both cell strains (1-way ANOVA, $p<0.0001$) in a manner qualitatively similar to calcein. In contrast to findings with calcein, levels of BSA uptake by each cell strain were significantly different, where wall-deficient cells took up much more BSA that the wild-type cells (2-way ANOVA, $p<0.0001$). The highest uptake level (C/C_0) achieved in wall-deficient cells (15%) is 7.5-fold larger than the highest uptake level achieved in wild-type cells (2%). This is consistent with the expectation that the cell wall significantly impedes transport of BSA and the hypothesis that electroporation does not increase cell wall permeability. It is also consistent with previous findings that DNA transfection of wall-deficient cells is greater than for wild-type cells (Brown et al. 1991; Shimogawara et al. 1998). Levels of BSA uptake in Figure 1B were generally lower than calcein uptake in Figure 1A for both strains (2-way ANOVA, $p<0.01$). Figure 1B also shows that cell viability decreased with increasing transmembrane potential in a manner similar to Figure 1A, which is consistent with the expectation that changing to a different inert uptake marker compound does not affect cell viability. In all cases, the highest intracellular calcein and BSA concentrations achieved were between 2 and 30% of the extracellular concentration, which represents on the order of 10^6 to 10^7 molecules per cell.

To understand these findings more fully, we examined histograms of cell fluorescence due to intracellular uptake among viable cells on a cell-by-cell basis. As shown in Figure 2, unelectroporated cells appear as a single population with low levels of background fluorescence. When wild-type cells were electroporated in the presence of calcein, the fluorescence distribution broadened and shifted to the right, which corresponds to a single population of cells with varying levels of uptake (Figure 2A). Wall-deficient cells showed calcein uptake distributions similar to wild-type cells (Figure 2B).

In contrast, BSA uptake by wild-type cells showed two subpopulations: a major sub-population with no uptake and a minor subpopulation with a distribution of low-level uptake (Figure 2C). This indicates that although calcein was taken up by essentially all cells that remained viable after electroporation, only a fraction of those cells took up BSA. Wall-deficient cells showed BSA uptake distributions similar to wild-type cells, although the second subpopulation had a larger fraction of cells and exhibited stronger fluorescence (Figure 2D). This shows that removal of the cell wall can increase BSA uptake, but a fraction of cells still did take up BSA during electroporation.

To quantitatively compare the distribution of cells among the various subpopulations, Figure 3 categorizes all cells exposed to electroporation as (i) viable cells with uptake (black bar), (ii) viable cells without uptake (gray bar), (iii) non-viable cells (striped bar) and (iv) lysed cells (white bar). Note that the height of the black-plus-gray bars shows the overall level of cell viability.

After electroporation of wild-type cells in the presence of calcein, all viable cells took up calcein and essentially all non-viable cells remained intact after electroporation, i.e., the fraction of lysed cells was indistinguishable from zero (1-way ANOVA, $p>0.05$) (Figure 3A). Electroporation of wall-deficient cells also showed uptake of calcein by all viable cells, but a significant fraction of non-viable cells were lysed as an increasing function of transmembrane potential (1-way ANOVA, $p<0.0001$) (Figure 3B).

Considering BSA uptake, only a small fraction of cells took up BSA, which occurred as an increasing function of transmembrane potential (1-way ANOVA, $p<0.0001$) (Figures 3C and 3D). The fraction of cells with uptake was significantly higher for wall-deficient cells than wild-type cells (2-way ANOVA, $p<0.05$), indicating that removing the cell wall increases both the fraction of cells with uptake and the number of molecules per cell. As expected, cell viability and lysis in Figures 3C and 3D showed behavior similar to Figures 3A and 3B, respectively.

In this study, we considered a broad range of electroporation conditions, including ones that killed large fractions of the cells, to more fully study the phenomena. Certainly, those conditions which kill most cells in the process of achieving intracellular delivery are less useful for applications, and electroporation at milder conditions is of greater relevance. Conditions useful for applications might include, for example, wild-type cells electroporated at a transmembrane potential of 0.06 V, which maintained more than 90% viability and essentially all of the cells took up significant amounts of calcein (Figure 3A).

Sonication

We next sought to determine the effects of sonication on transport across cells with and without cell walls as a function of molecular size and ultrasound conditions. If our original hypothesis is correct, there should be significant differences between uptake caused by electroporation and sonication. We expect that both calcein and BSA should be delivered into wild-type cells to similar extents, because we hypothesize that ultrasound non-selectively disrupts cell membrane and cell wall structure to transport both small molecules and macromolecules into cells.

Considering calcein first, Figure 4A shows that calcein uptake increased at elevated ultrasound energy exposure for wild-type cells (1-way ANOVA, $p<0.0001$), which is consistent with previously observed behavior in other cell types (Guzman et al. 2001a; Keyhani et al. 2001). However, wall-deficient cells exhibited no uptake (1-way ANOVA, $p>0.05$). This difference may be explained by examining the viability data, which shows that cell viability decreased with increasing energy exposure for both cell strains (1-way ANOVA, $p<0.0001$) and that the wall-deficient cells were generally more easily killed than wild-type cells (2-way ANOVA, $p<0.05$). The almost complete killing of wall-deficient cells at relatively mild ultrasound exposures suggests that wall-deficient cells cannot survive disruption by sonication sufficient to permit uptake of calcein, whereas wild-type cells are capable of recovery.

Considering BSA, Figure 4B shows that BSA uptake increased at elevated acoustic energy exposure for wild-type cells (1-way ANOVA, $p<0.0001$) to levels similar to calcein uptake. The maximum uptake levels for both molecules were 30 – 35%. This result contrasts with the effects of electroporation; although calcein uptake levels were similar, the maximum uptake levels of BSA during electroporation of wild-type cells are 17-fold smaller than during sonication. This is an important finding in support of our hypothesis that sonication transports molecules across both cell membranes and cell walls.

During sonication, uptake of calcein and BSA were not identical; BSA uptake did not occur until larger acoustic energy exposures than calcein uptake. Calcein uptake at 25 J/cm^2 was statistically different from 0 J/cm^2 (Student's t-test, $p<0.0001$), whereas BSA uptake did not become statistically different from 0 J/cm^2 until 100 J/cm^2 was applied (Student's t-test, $p<0.0001$). Uptake of BSA by wall-deficient cells was not examined, given that calcein uptake did not occur and most wall-deficient cells were killed by sonication. Figure 4B also shows that cell viability decreased with increasing acoustic energy exposure in a manner similar to Figure 4A.

Histograms of intracellular uptake among viable cells show heterogeneous responses similar to results seen during sonication of other cell types (Figure 5) (Guzman et al. 2001b). Figure 5A shows that when wild-type cells were sonicated in the presence of calcein, one subpopulation appeared to be unaffected, a second subpopulation had somewhat increased uptake, and a third subpopulation had dramatically increased uptake. BSA uptake by wild-type cells showed similar behavior, although the third subpopulation was not evident (Figure 5C). As expected from Figure 4, wall-deficient cells showed no uptake (Figure 5B).

During sonication of wild-type cells, a large fraction of viable cells took up calcein and a comparable fraction took up BSA (Figures 6A and 6C), which is similar to observations in other cell types (Guzman et al. 2001b). This is consistent with our hypothesis that cells that were disrupted sufficiently for calcein uptake could also take up BSA. Figure 6B shows that no wall-deficient cells took up calcein. Examining viability shows that increasing acoustic energy exposure for wild-type cells increased both loss of cell viability and the fraction of cells that were lysed (1-way ANOVA, $p<0.0001$) (Figures 6A and 6C). Among wall-deficient cells, essentially all non-viable cells were lysed, i.e., the fraction of non-viable, non-lysed cells was indistinguishable from zero (1-way ANOVA, $p>0.05$). This indicates that the cell wall is needed to prevent cell lysis after sonication.

DISCUSSION

Electroporation vs. Sonication Mechanisms

The primary objective of this study was to test the hypothesis that electroporation primarily transports molecules across cell membranes, because its mechanism is known to be specific to lipid bilayer disruption (Jaroszeski et al. 2000; Weaver and Chizmadzhev 1996), whereas sonication transports molecules across both cell membranes and cell walls, because it non-specifically disrupts cell-surface barriers. The data from this study generally support this hypothesis. The presence of a cell wall significantly reduced intracellular delivery of BSA during electroporation, but generally did not reduce BSA uptake during sonication.

Further examination of the electroporation data shows that even in the presence of a cell wall, some BSA delivery was possible, and in the absence of a cell wall, BSA delivery was still less than calcein delivery. This apparent inconsistency is probably due to an oversimplification of the interpretation. Although wild-type cells are surrounded by a multilayered cell wall, this wall expands during cell growth (Voigt 1985; Voigt 1986), which transiently increases the pore size of the wall and may thereby permit transport of macromolecules, such as BSA. The cell wall barrier is composed of an insoluble, crystalline hydroxyproline-rich glycoprotein framework and several chaotrope-soluble, hydroxyproline-containing glycoproteins (Monk et al. 1983). Holes formed during cell growth are repaired by the addition of newly synthesized soluble glycoproteins. In contrast, wall-deficient cells do not have a complete cell wall because they lack the major class of glycoprotein that forms the insoluble layer, but still have other proteins present on the cell surface (Monk et al. 1983), which could limit uptake of macromolecules such as BSA.

Further examination of the sonication data shows that although calcein and BSA uptake levels were similar at large energy exposures, BSA uptake was much less facile at lower energies. This difference can be explained if low energy exposures can disrupt the cell membrane and thereby permit entry of calcein, but energies greater than 100 J/cm^2 are needed to disrupt the cell wall as well, so that BSA can readily enter the cell. An additional explanation could involve small disruptions to the cell membrane and the cell wall at low energies that permit transport of calcein ($r = 0.6$ nm), but impede transport of BSA ($r = 3.5$ nm), and larger disruptions at higher energies that permit transport of both calcein and BSA.

It is consistent with previous work on electroporation that this phenomenon should occur only in the cell membrane and not affect the cell wall. Electroporation is believed to occur when a few hundred millivolts are applied across a lipid bilayer, which forces ions and water into the membrane's hydrophobic tailgroup region and leads to a structural rearrangement that yields a metastable transmembrane pore (Weaver and Chizmadzhev 1996). The specific hydrophilic-hydrophobic sandwich structures present in a lipid bilayer, in combination with its fluidity, are generally necessary for the reversible electroporation phenomenon. For this reason, electroporation occurs universally in lipid bilayers, both artificial and biological, and has not been reported in other types of membranes (Chang et al. 1992). This phenomenon contrasts with dielectric breakdown, which involves an irreversible disruption of membrane structure that does not require the fluidity of a lipid bilayer and is observed in many materials.

Irreversible dielectric breakdown of the cell wall could have occurred in this study, but apparently did not. This should be expected, because the cell wall offers a much smaller electrical resistance than the cell membrane, which thereby concentrates the electric field within the cell membrane and results in a much smaller electric field within the cell wall. This provides a further explanation for electroporation's effects targeted to the cell membrane.

Although much less is known about how sonication delivers molecules into cells, evidence suggests that its mechanism is significantly different from electroporation. Cavitation bubble formation, oscillation, and collapse during sonication appears to be critical for intracellular uptake, where emission of a shock wave and/or a high-velocity fluid jet from a collapsing bubble may be key event (Miller et al. 1996; Prentice et al. 2005). The resulting mechanical impact with the cell has been proposed to rip open the plasma membrane (of mammalian cells), which is subsequently resealed by the cell (Schlicher et al. 2006). This type of non-specific mechanical event is not expected to target lipid bilayers and could similarly affect the cell wall.

An additional difference between sonication and electroporation is that sonication is believed to create pores up to 1 μm in size (Schlicher et al. 2006), which contrasts with the 1 – 10 nm size pores created by electroporation (Jaroszeski et al. 2000; Weaver and Chizmadzhev 1996). This may also contribute to why sonication more efficiently delivered BSA macromolecules into cells.

Phenomenological Observations and Interpretations

Calcein delivery during electroporation of wild-type cells was characterized by two outcomes: viable cells with uptake and non-viable cells that were not lysed (Figure 3). Notably, viable cells without uptake and non-viable cells that were lysed were generally not present. This observation is similar to findings with mammalian cells (Canatella et al. 2001), which lack a cell wall, but have other cytoskeletal structures to provide strength. Calcein delivery to wall-deficient cells had the same two outcomes, as well as non-viable cells that were lysed (Figure 3) This observation is similar to findings with mammalian red blood cells (Prausnitz et al. 1993), which have fewer mechanical supporting structures than nucleated mammalian cells (Secomb 1991).

Calcein (and BSA) delivery during sonication of wild-type cells was characterized by all four of the possible outcomes (Figure 6). This heterogeneity has also been observed for mammalian cells and explained by a cavitation-based mechanism that releases energy heterogeneously in time and space (Guzman et al. 2003). Cells located immediately next to a collapsing cavitation bubble are lysed; cells located further away, and thereby experiencing a smaller local energy flux, are killed but remain non-lysed; cells located still further away have the desirable outcome of uptake while maintaining viability; and cells located beyond the "blast radius" are unaffected.

In contrast to wild-type cells, sonication of wall-deficient cells was generally characterized by just two outcomes: viable cells without uptake and non-viable cells that were lysed (Figure 6). This could be explained by an inability of wall-deficient cells to repair membrane defects. In the absence of a cell wall, even a small tear could grow in size until the cell lysed. In contrast, the presence of a cell wall could constrain the growth of a disruption by maintaining cell shape and thereby permit the cell to repair the defect. This may be related to our observation that mammalian red blood cells also do not take up molecules following sonication, probably due to an inability to reseal disruptions (Schlicher et al. 2006).

Applications to Plant Biotechnology

Many applications in plant biotechnology would benefit from improved methods to deliver molecules into plant cells. Electroporation is already a well-established technique for intracellular delivery, especially of genes. This study explicitly shows the limitations of trying to deliver macromolecules into cells with intact cell walls and demonstrates why delivery to wall-deficient protoplasts is known to be more effective (albeit less useful to applications). For this reason, sonication may provide a more useful tool for plant biotechnology as a technique that can deliver large numbers of macromolecules into intact plant cells, assuming that findings with algal cells can be extrapolated to higher plant cells.

Optimizing a delivery method requires identifying appropriate electroporation and sonication parameters. This study showed that increasing transmembrane voltage during electroporation in the presence of calcein increased the number of molecules per cell and decreased cell viability (Figure 1). Thus, there is a trade-off between uptake and viability that can be optimized for different applications. In contrast, increasing acoustic energy exposure during sonication in the presence of calcein did not change the number of molecules per cell, but did decrease cell viability (Figure 4). Thus, applications that seek to deliver molecules into viable cells should be optimized by low energies that are just above the cavitation threshold for bioeffects (not determined in this study). The lowest non-zero energy exposure used in this study (25 J/cm^2) delivered on the order of 10^6 molecules per cell and cell viability exceeded 75% (Figure 4). Studies in mammalian cells suggest that still lower energies can deliver similar numbers of molecules with viabilities that exceed 90% (Guzman et al. 2001a;Keyhani et al. 2001). Additional studies are needed for further optimization of conditions for specific applications.

While it would be ideal to avoid killing cells, applications in, for example, in vitro plant biotechnology can often tolerate loss of some cells. Frequently, it is more important to obtain a pure population of cells, even if just a fraction of the original cells, that can be cultured to produce many more cells. Thus, loss of cell viability associated with high levels of uptake is not always problematic for in vitro applications.

Although this study has direct relevance to protein delivery to algal cells, some questions remain about its ability to predict, for example, gene delivery to higher plants. Given the differences between the cell wall and other physiological and structural aspects of lower and higher plants, additional experiments are needed to study the effects of electroporation and, especially, sonication of higher plant cells. Moreover, although calcein and BSA span a broad range of molecular masses, delivery characteristics of other molecules may be different, especially for molecules larger than BSA that may have even greater difficulty crossing the cell wall.

CONCLUSIONS

In this study, experiments were carried out to determine the effect of electroporation transmembrane potential, acoustic energy exposure, uptake molecule size, and the presence of a cell wall on intracellular uptake and cell viability. We believe this is the first study to

quantitatively compare intracellular uptake due to electroporation and sonication in a direct fashion. It is also the first study to examine the effects of sonication on intracellular delivery to algal cells. Overall, intracellular uptake was found to increase and cell viability was found to decrease with increasing transmembrane potential during electroporation and acoustic energy exposure during sonication. Electroporation-mediated uptake showed size selectivity, where essentially all viable cells took up calcein, but only a small fraction of wild-type cells (i.e., with cell walls) took up BSA. Cells lacking a cell wall took up as much as 7.5-fold more BSA than wild-type cells. In contrast, ultrasound-mediated uptake showed less size selectivity, where calcein and BSA entered cells with similar ease. Maximum BSA uptake during sonication of wild-type cells was 17-fold greater than during electroporation. Absence of a cell wall decreased cell viability after electroporation and sonication apparently due to an increase in cell lysis. Sonication of wall-deficient cells caused cell lysis so extensively that essentially all wall-deficient cells affected by ultrasound were lysed.

Together, these observations suggest that the cell wall provides physical strength to cells that impedes macromolecule uptake during electroporation, but is a much smaller barrier to transport during sonication. We conclude that electroporation primarily transports molecules across cell membranes, because its mechanism is specific to lipid bilayer disruption, whereas sonication transports molecules across both cell membranes and cell walls, because it non-specifically disrupts cell-surface barriers. For this reason, sonication may provide a useful technique to deliver macromolecules into plant cells.

Acknowledgements

We thank Andrew McNamara for assistance carrying out experiments; Johnafel Crowe for support with flow cytometry and confocal microscopy; Dr. Bao Phan, Dr. Taraknath Chakravarthy, and Teresa Vales for help with cell culture; and Dr. Elizabeth Harris for advice and guidance regarding *C. reinhardtii*. This work was supported in part by the National Science Foundation, National Institutes of Health, and IPST member company support.

References

Adair WS, Steinmetz SA, Mattson DM, Goodenough UW, Heuser JE. Nucleated assembly of Chlamydomonas and Volvox cell walls. J Cell Biol 1987;105(5):2373–2382. [PubMed: 3680387]

Bekeredjian R, Grayburn PA, Shohet RV. Use of ultrasound contrast agents for gene or drug delivery in cardiovascular medicine. J Am Coll Cardiol 2005;45(3):329–335. [PubMed: 15680708]

Birch RG. Plant transformation: problems and strategies for practical application. Ann Rev Plant Physiol Plant Mol Biol 1997;48:297–326. [PubMed: 15012265]

Brown LE, Sprecher SL, Keller LR. Introduction of exogenous DNA into Chlamydomonas reinhardtii by electroporation. Mol Cell Biol 1991;11:2328–2332. [PubMed: 2005916]

Canatella P, Black M, Bonnichsen D, McKenna C, Prausnitz M. Tissue electroporation: quantification and analysis of heterogeneous transport in multicellular environments. Biophys J 2004;86:3260–3268. [PubMed: 15111439]

Canatella PJ, Karr JF, Petros JA, Prausnitz MR. Quantitative study of electroporation-mediated molecular uptake and cell viability. Biophys J 2001;80:755–764. [PubMed: 11159443]

Carpita N, Gibeaut D. Structural models of primary cell walls in flowering plants: consistency of molecular structure with the physical properties of the walls during growth. Plant J 1993;3:1–30. [PubMed: 8401598]

Chang, DC.; Chassy, BM.; Saunders, JA.; Sowers, AE., editors. Guide to Electroporation and Electrofusion. Academic Press; New York: 1992.

Cochran SA, Prausnitz MR. Sonoluminescence as an indicator of cell membrane disruption by acoustic cavitation. Ultrasound Med Biol 2001;27(6):841–850. [PubMed: 11516544]

Davis LI. The nuclear pore complex. Annu Rev Biochem 1995;64:865–896. [PubMed: 7574503]

Edwards DA, Prausnitz MR, Langer R, Weaver JC. Analysis of enhanced transdermal transport by skin electroporation. J Control Release 1995;34:211–221.

Foster, KR.; Schwann, HP. Dielectric properties of tissues. In: Polk, C.; Postow, E., editors. CRC Handbook of Biological Effects of Electromagnetic Fields. CRC Press; Boca Raton: 1986. p. 27-96.

Gad AE, Rosenberg N, Altman A. Liposome-mediated gene delivery into plant cells. Physiol Plant 1990;79:177–183.

Gift EA, Weaver JC. Observation of extremely heterogeneous electroporative molecular uptake by *Saccharomyces cerevisiae* which changes with electric field pulse amplitude. Biochim Biophys Acta 1995;1234:52–62. [PubMed: 7880860]

Guzman HR, McNamara AJ, Nguyen DX, Prausnitz MR. Bioeffects caused by changes in acoustic cavitation bubble density and cell concentration: a unified explanation based on cell-to-bubble ratio and blast radius. Ultrasound Med Biol 2003;29(8):1211–1222. [PubMed: 12946524]

Guzman HR, Nguyen DX, Khan S, Prausnitz MR. Ultrasound-mediated disruption of cell membranes I: Quantification of molecular uptake and cell viability. J Acoust Soc Am 2001a;110:588–596. [PubMed: 11508983]

Guzman HR, Nguyen DX, Khan S, Prausnitz MR. Ultrasound-mediated disruption of cell membranes II: Heterogeneous effects on cells. J Acoust Soc Am 2001b;110:597–606. [PubMed: 11508985]

Guzman HR, Nguyen DX, McNamara AJ, Prausnitz MR. Equilibrium loading of cells with macromolecules by ultrasound: Effects of molecular size and acoustic energy. J Pharm Sci 2002;91 (7):1693–1701. [PubMed: 12115831]

Harris, EH. The Chlamydomonas Source Book: A Comprehensive Guide to Biology and Laboratory Use. Academic Press; New York: 1989.

Heller LC, Heller R. In vivo electroporation for gene therapy. Hum Gene Ther 2006;17(9):890–897. [PubMed: 16972757]

Hyams J, Davies D. Induction and characterization of cell-wall mutants of Chlamydomonas reinhardi. Mutat Res 1972;14:381–389.

Jaroszeski, MJ.; Heller, R.; Gilbert, R., editors. Electrochemotherapy, Electrogenetherapy, and Transdermal Drug Delivery. Humana Press; Totowa, NJ: 2000.

Joersboe M, Brunstedt J. Direct gene transfer to plant protoplasts by mild sonication. Plant Cell Reports 1990;9:207–210.

Kaeppler HF, Gu W, Somers DA, Rines HW, Cockburn AF. Silicon carbide fiber-mediated DNA delivery into plant cells. Plant Cell Rep 1990;8:415–418.

Keyhani K, Guzman HR, Parsons A, Lewis TN, Prausnitz MR. Intracellular drug delivery using low-frequency ultrasound: quantification of molecular uptake and cell viability. Pharm Res 2001;18(11): 1514–1520. [PubMed: 11758757]

Knox JP. Plant cell adhesion. Plant J 1992;2:137–141.

Leighton, TG. The Acoustic Bubble. Academic Press; London: 1994.

Liu J, Lewis TN, Prausnitz MR. Non-invasive assessment and control of ultrasound-mediated membrane permeabilization. Pharm Res 1998;15(6):920–926.

Lui Y, Yang H, Sakanish A. Ultrasound: mechanical gene transfer into plant cells by sonoporation. Biotech Adv 2006;24(1):1–16.

Miller MW, Miller DL, Brayman AA. A review of in vitro bioeffects of inertial ultrasonic cavitation from a mechanistic perspective. Ultrasound Med Biol 1996;22:1131–1154. [PubMed: 9123638]

Mir LM, Morsli N, Garbay JR, Billard V, Robert C, Marty M. Electrochemotherapy: a new treatment of solid tumors. J Exp Clin Cancer Res 2003;22(4 Suppl):145–148. [PubMed: 16767921]

Monk BC, Adair WS, Cohen RA, Goodenough UW. Topography of Chlamydomonas: fine structure and polypeptide components of the gametic flagellar membrane surface and the cell wall. Planta 1983;158:517–533.

Neuhaus G, Spangenberg G. Plant transformation by microinjection techniques. Physiol Plant 1990;79:213–217.

Nickoloff, JA., editor. Plant Cell Electroporation and Electrofusion Protocols. Humana Press; Totowa, NJ: 1995.

Paliwal S, Mitragotri S. Ultrasound-induced cavitation: applications in drug and gene delivery. Expert Opin Drug Deliv 2006;3(6):713–726. [PubMed: 17076594]

Pitt WG, Husseini GA, Staples BJ. Ultrasonic drug delivery -- a general review. Expert Opin Drug Deliv 2004;1(1):37–56. [PubMed: 16296719]

Potrykus J, Shillito RD. Protoplasts: Isolation, culture, plant regeneration. Methods Enzymol 1986;118:549–578.

Prausnitz MR, Lau BS, Milano CD, Conner S, Langer R, Weaver JC. A quantitative study of electroporation showing a plateau in net molecular transport. Biophys J 1993;65(July):414–422. [PubMed: 7690262]

Prentice P, Cuschieri A, Dholakia K, Prausnitz M, Campbell P. Membrane disruption by optically controlled microbubble cavitation. Nature Physics 2005;1:107–110.

Schlicher RK, Radhakrishna H, Tolintino TP, Apkarian RP, Zarnitsyn V, Prausnitz MR. Mechanism of intracellular delivery by acoustic cavitation. Ultrasound Med Biol 2006;32:915–924. [PubMed: 16785013]

Secomb TW. Red blood cell mechanics and capillary blood rheology. Cell Biophys 1991;18(3):231–251. [PubMed: 1726534]

Sharma K, Bhatnagar-Mathur P, Thorpe T. Genetic transformation technology: status and problems. In Vitro Cell Dev Biol Plant 2005;41:101–112.

Shimogawara K, Fujiwara S, Grossman A, Usuda H. High-efficiency transformation of Chlamydomonas reinhardtii by electroporation. Genetics 1998;148(4):1821–1828. [PubMed: 9560396]

Songstad DD, Somers DA, Griesbach RJ. Advances in alternative DNA delivery techniques. Plant Cell Tissue Organ Cult 1995;40:1–15.

Sueoka N. Mitotic replication of deoxyribonucleic acid in Chlamydomonas reinhardi. Proc Natl Acad Sci USA 1960;46:83–91. [PubMed: 16590601]

Taylor NJ, Fauquet CM. Microparticle bombardment as a tool in plant science and agricultural biotechnology. DNA Cell Biol 2002;21(12):963–977. [PubMed: 12573053]

Trick HN, Finer JJ. SAAT: sonication-assisted Agrobacterium-mediated transformation. Transgenic Res 1997;6:329–336.

Voigt J. Macromolecules released into the culture medium during the vegetative cell cycle of the unicellular green alga Chlamydomonas reinhardtii. Biochem J 1985;226:259–268. [PubMed: 3977869]

Voigt J. Biosynthesis and turnover of cell wall glycoproteins during the vegetative cell cycle of Chlamydomonas reinhardtii. Z Naturforsch 1986;41c:885–896.

Weaver JC, Chizmadzhev YA. Theory of electroporation: a review. Bioelectrochem Bioenerget 1996;41:135–160.

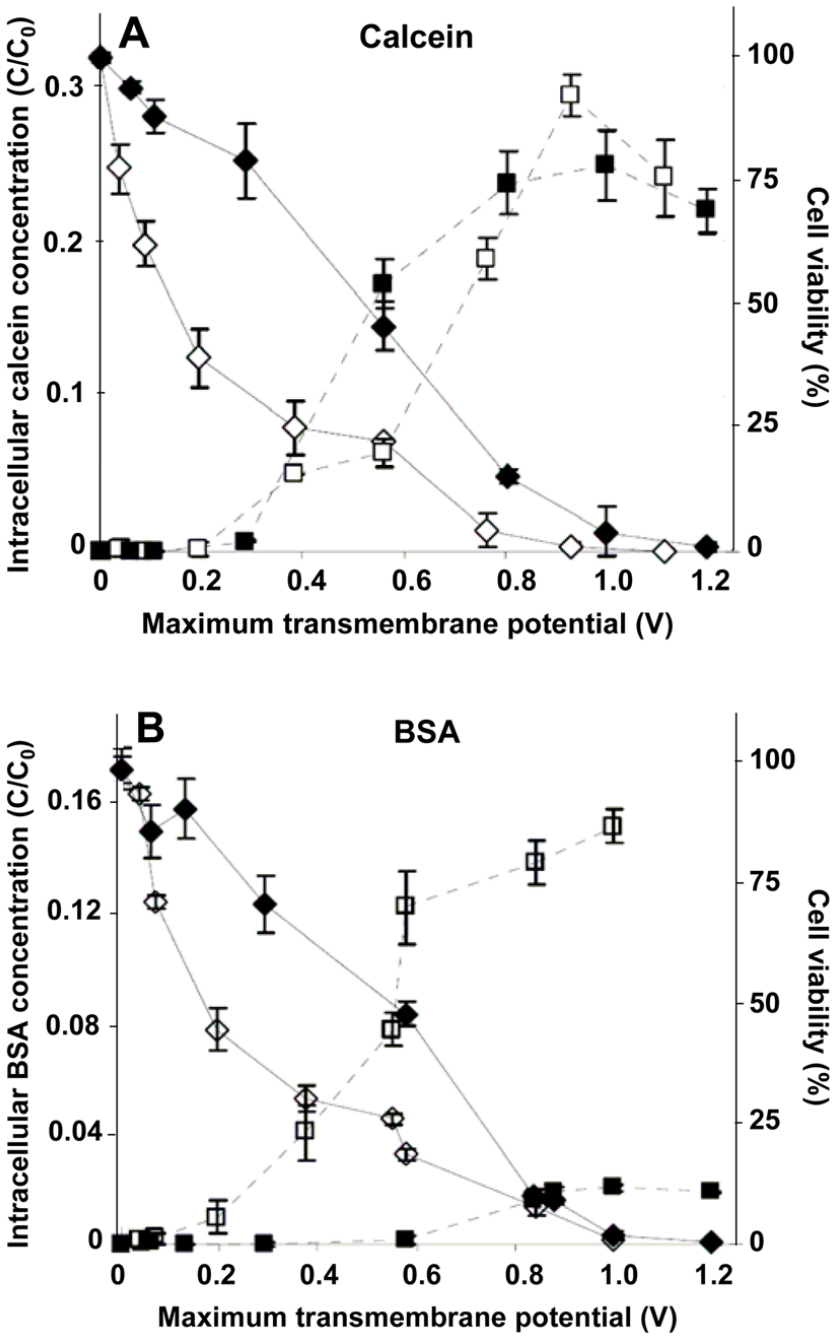

Figure 1.

Influence of the cell wall on intracellular uptake and cell viability as a function of transmembrane potential during electroporation. The normalized intracellular concentration of a small molecule, calcein (A), and a macromolecule, BSA (B), is shown versus the nominal, applied, maximum, transmembrane potential for two 1-ms electroporation pulses. For the same population of cells, the cell viability is also shown. The black and white symbols represent data from the wild-type and wall-deficient algal cells, respectively. The square and diamond symbols represent intracellular concentration and cell viability, respectively. These data show that although both cell strains took up similar amounts of calcein, wild-type cells took up significantly less BSA than wall-deficient cells.

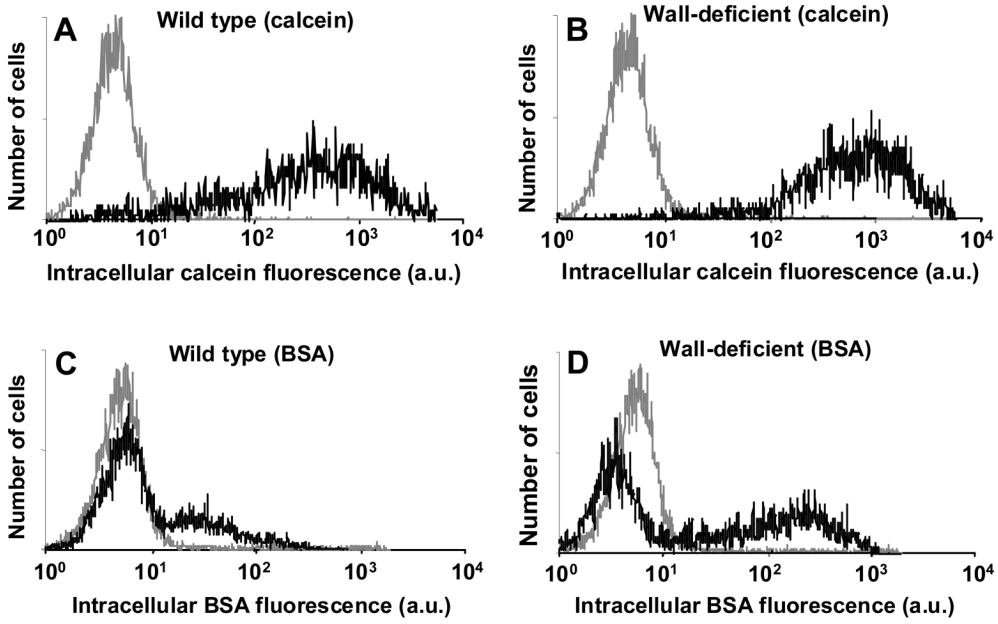

Figure 2.

Histograms of intracellular uptake on a per-cell basis measured by cell fluorescence representative of the data shown in Figure 1. Uptake of calcein (A, B) and BSA (C, D) is shown in wild-type (A, C) and wall-deficient (B, D) cells. In each graph, the gray curve represents fluorescence of control cells and the black curve represents fluorescence of electroporated cells. Intracellular fluorescence is reported in arbitrary flow cytometry units. Each histogram contains data from 20,000 cells.

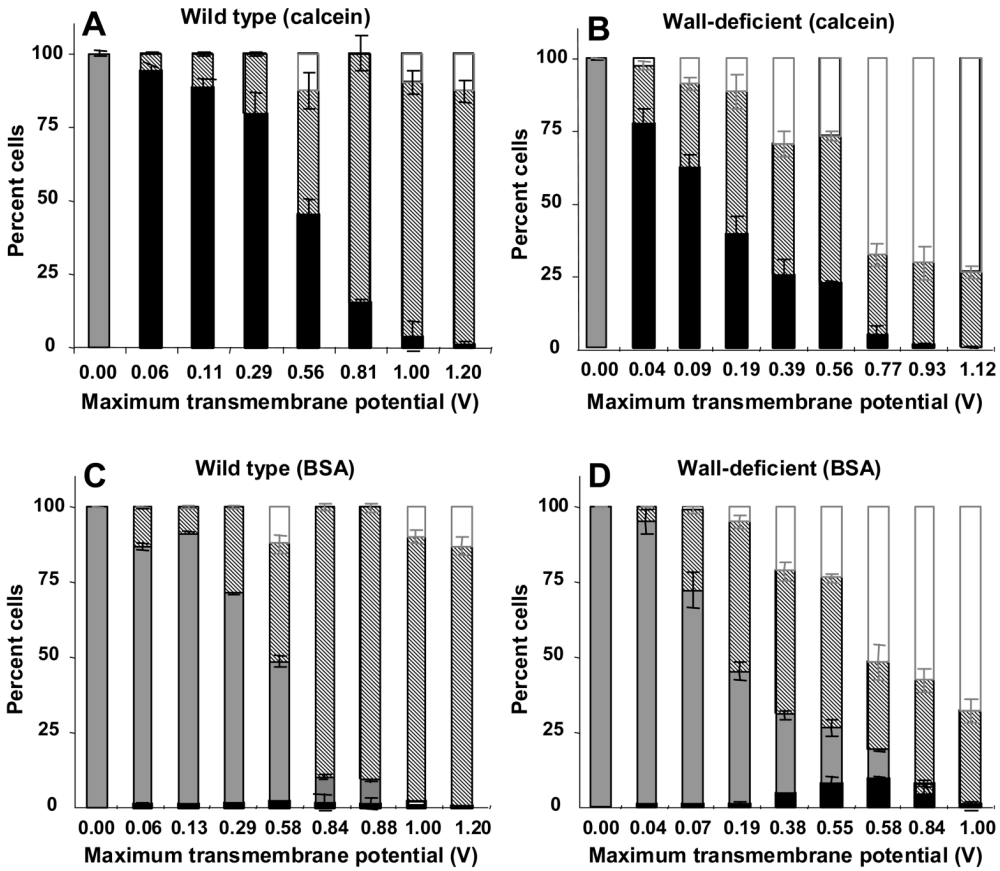

Figure 3.

Influence of the cell wall on intracellular uptake and cell viability as a function of transmembrane potential during electroporation. Uptake of calcein (A, B) and BSA (C, D) is shown in wild-type (A, C) and wall-deficient (B, D) cells. All cells exposed to electroporation have been categorized as (i) viable cells with uptake (black bar), (ii) viable cells without uptake (gray bar), (iii) non-viable cells (striped bar) and (iv) lysed cells (white bar). Note that the height of the black-plus-gray bars shows the overall level of cell viability. This figure was generated using data from Figure 1 that were reanalyzed using histograms like those shown in Figure 2. This analysis demonstrates that essentially all electroporated cells took up calcein, but only some cells took up BSA, where a larger fraction of wall-deficient cells took up BSA than wild-type cells.

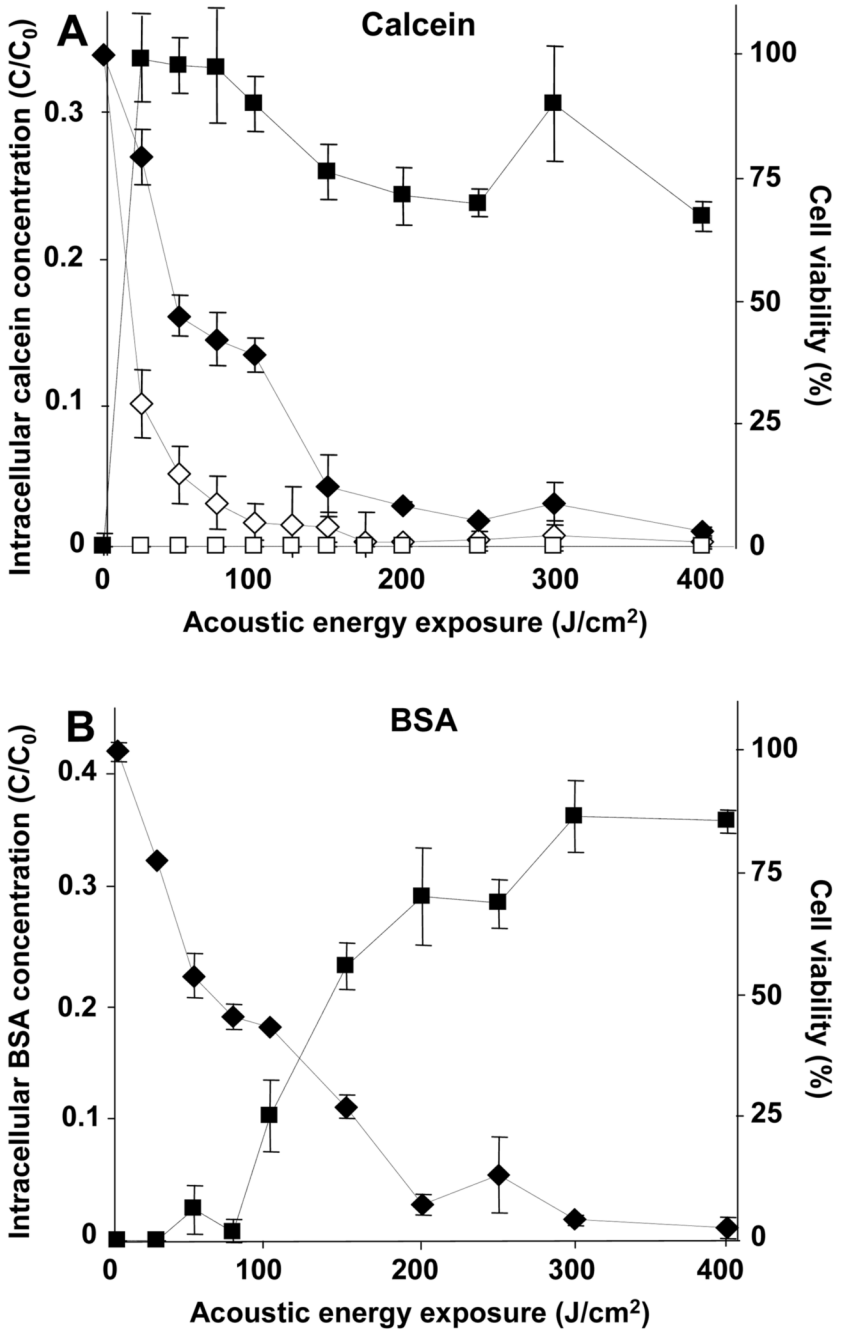

Figure 4.

Influence of the cell wall on intracellular uptake and cell viability as a function of energy exposure during sonication. The normalized intracellular concentration of a small molecule, calcein (A), and a macromolecule, BSA (B), is shown versus acoustic energy exposure. For the same population of cells, the cell viability is also shown. The black and white symbols represent data from the wild-type and wall-deficient algal cells, respectively. The square and diamond symbols represent intracellular concentration and cell viability, respectively. These data show that wild-type cells exposed to sonication take up large amounts of BSA, which contrasts with the lesser effects of electroporation, and that wall-deficient cells are easily killed by sonication and do not take up molecules at all. In (B), data are not shown for BSA uptake

in wall-deficient cells, because (A) demonstrated that wall-deficient cells do not take up calcein and therefore are not expected to take up BSA either.

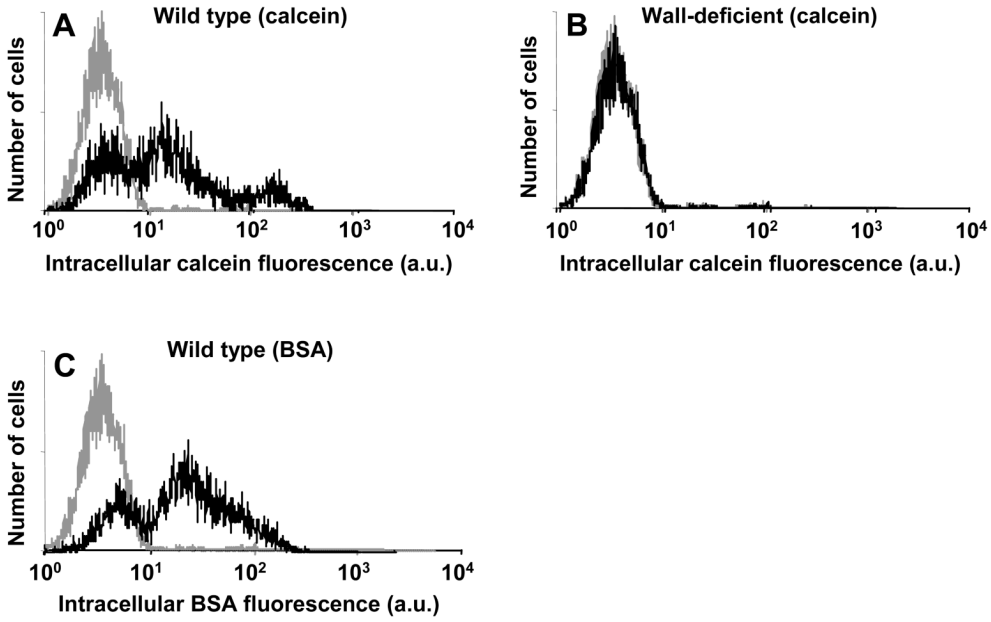

Figure 5.

Histograms of intracellular uptake on a per-cell basis measured by cell fluorescence representative of the data shown in Figure 4. Uptake of calcein (A, B) and BSA (C) is shown in wild-type (A, C) and wall-deficient (B) cells. In each graph, the gray curve represents fluorescence of control cells and the black curve represents fluorescence of sonicated cells. Intracellular fluorescence is reported in arbitrary flow cytometry units. Each histogram contains data from 20,000 cells.

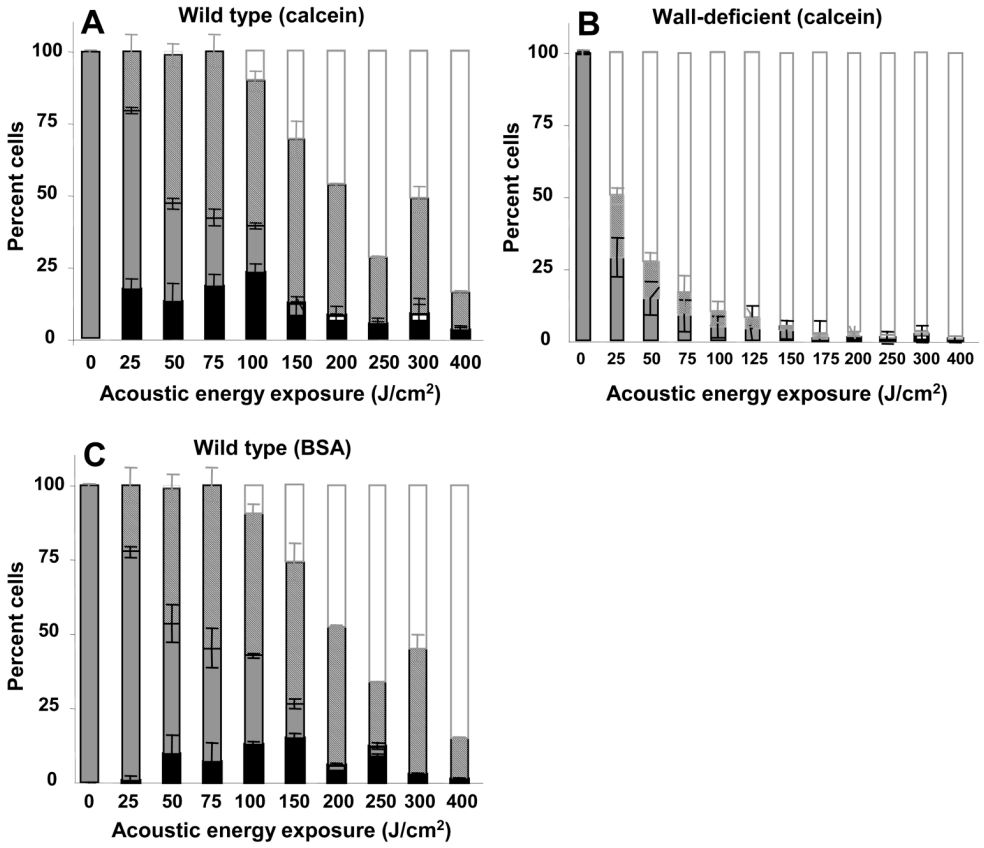

Figure 6.

Influence of the cell wall on intracellular uptake and cell viability as a function of energy exposure during sonication. Uptake of calcein (A, B) and BSA (C) is shown in wild-type (A, C) and wall-deficient (B) cells. All cells exposed to sonication have been categorized as (i) viable cells with uptake (black bar), (ii) viable cells without uptake (gray bar), (iii) non-viable cells (striped bar) and (iv) lysed cells (white bar). Note that the height of the black-plus-gray bars shows the overall level of cell viability. This figure was generated using data from Figure 4 that were reanalyzed using histograms like those shown in Figure 5. This analysis shows that similar fractions of wild-type and wall-deficient cells took up calcein and BSA, but essentially no wall-deficient cells took up molecules.